Name: Ju Young Ahn
Group 5.
04/28/16

Critical Review: Self-calibration of Cone-beam CT Geometry Using 3D–2D Image Registration.

Ouadah, S., J. W. Stayman, G. J. Gang, T. Ehtiati, and J. H. Siewerdsen. "Self-calibration of Cone-beam CT Geometry Using 3D–2D Image Registration."Physics in Medicine and Biology Phys. Med. Biol. 61.7 (2016): 2613-632. Web.

Project Overview

The aim of our project is to develop user-friendly interfaces to simulate fluoroscopic views of mobile C-arm. C-arm is an X-ray imaging device with flexible positioning of X-ray source. Because of its multiple degree of freedom (DoF) and flexibility, C-arm is widely used for diagnostic imaging or surgical procedures in many areas including orthopedic surgeries.

However, surgeons who utilize C-arm during surgical procedures often encounter a challenge called "fluoro-hunting." Surgeons often take multiple fluoroscopic shots in order to set an optimal fluoroscopic view that they desire. This procedure is often time-consuming, exposes more radiation to both physicians and patients, is physically cumbersome and has safety issues.

In order to solve problems associated with "fluoro-hunting," we propose to develop user-friendly interfaces to locate an optimal C-arm source position with a digitally reconstructed radiograph (DRR) generated from preoperative 3D data. Because no fluoroscopic shots are required using DRR, our solution has several advantages including less time consumption, less radiation exposure, and less user-variability/ more consistency.

Paper Selection

The paper selected "Self-calibration of Cone-beam CT Geometry Using 3D-2D Image Registration" by Ouadah *et al* proposes a novel method called "self-calibration" to compute geometric calibration for any arbitrary source-detector position of complex orbits from mobile C-arm. The method they use to perform geometric calibration is to register 2D projection data to a previously acquired 3D image, thereby achieving 3D-2D image registration. Since one of our maximum deliverables is to implement 3D-2D image registration for patient-CT registration, this paper offers a guidance to understand the general framework of our future work. Moreover, geometric calibration for an arbitrary source-detector position is necessary for our project because our C-arm produce nonisocentric orbit and an oblique change in source-detector position requires geometric calibration for accurate DRR production.

Problem Statement/ Introduction

A geometric calibration is composed of geometric relationship between the x-ray source and detector and errors associated with calibration often result in image artifacts such as blur, distortion, and streaks. This paper tries to solve the challenge that even though there are several methods to reliably calibrate for nominal circular orbits, it is not practical to calibrate for all anticipated orbits and these methods do not apply well to non-circular orbits. Also, this paper addresses the problem that calibration might become out-of-date as system geometry might change over time and as orbits are not completely reproducible due to vibration of C-arm. Moreover, this paper argues that mobile C-arm is capable of departing from a circular orbit for better field-of-view or better image quality (resulting in a non-circular orbits). This patient-specific nature of the orbit causes inability to calibrate for all possible trajectories of the system and this paper tests feasibility of self-calibration method to solve this problem.

In short, this paper proposes "an online geometric calibration method that registers the 2D projection data to a previously acquired 3D image of the subject, providing a 'self-calibration' of the system." An online geometric calibration utilizes the 2D scan projection data as fluoroscopic images are taken with knowledge of patient-specific 3D data. 3D-2D image registration is performed to solve affine transformation associated with each projection, thereby deriving the system geometry for each acquisition. Moreover, this paper argues that this method is less computationally intense in comparison to iterative image reconstruction techniques.

Name: Ju Young Ahn
Group 5.
04/28/16

Technical Approach - Overview

An overall technical approach is following: for each projection, the registration initialized, 3D-2D image registration is performed, and outliers are checked (for the purpose of relatively short review paper and relevance of my project, I will not discuss method for outlier checking). Once system geometry is found for all projections, 3D volume is reconstructed.

Technical Approach - 1) Initialization

For the first projection (i = 1), PM (projection matrix) is initialized from coarse estimation based on geometry; $T_{d,z}$ and $T_{s,z}$ are initialized as object-detector distance and detector-source distance. For the orientation, brute force (rotate 90° about the 3 cardinal axes) is used to check for all possible 24 orientations and whichever yielded maximum similarity is selected as PM_1.

For the second view (i = 2), PM is initialized using PM1

Then, for projections i = 3,...,N, PM is initialized as $PM_{predict}$, which is based on the geometries of the previous two views. $PM_{predict}$ is a linear extrapolation using detector position and rotation (T_d and R_d) in the 6 DoF. In more detail, $PM_{predict}$ is computed by solving the transformation from $(T_d, R_d)^{i-2}$ to $(T_d, R_d)^{i-1}$. (Refer to *figure 1*.)

Following blue lines,

$$ {}^{d^{i-1}}T_{d^{i-2}} = {}^{d^{i-1}}T_{CT}\left({}^{d^{i-2}}T_{CT}\right)^{-1}. $$

(where ${}^{d^{i-1}}T_{CT}$ is the homogeneous transformation from 3D CT coordinates to 3D detector coordinate for the *(i-1)*th view

and ${}^{d^{i-1}}T_{d^{i-2}}$ is the homogeneous transformation from 3D detector coordinates for the *(i-2)*th view to *(i-1)*th view)

Then, this transformation is used to obtain a prediction for $(T_d, R_d)^i$.

Following red lines,

$$ {}^{d^{i}}T_{CT} = {}^{d^{i-1}}T_{d^{i-2}}\left({}^{d^{i-1}}T_{CT}\right), $$

which is used as initialization for *i*th view registration.

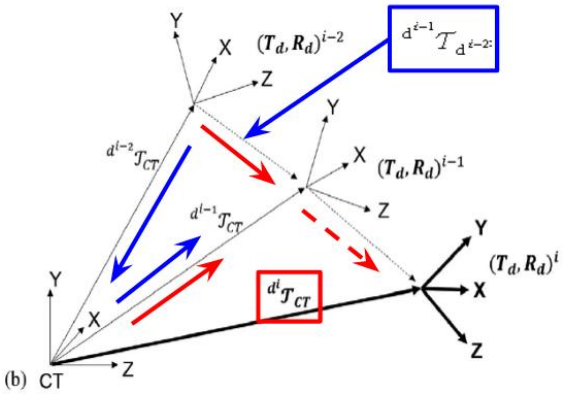

<Figure 1. Initialization>

Technical Approach - 2) 3D-2D Image Registration

3D-2D image registration is based on the work of Otake et al. This method utilizes normalized gradient information (NGI) as a robust similarity metric with the covariance matrix adaptation-evolution strategy (CMA-ES) optimizer. NGI is computed between the CT (I_M) and the DRR generated (I_F).

$$\mathrm{NGI}(\mathrm{I_F}, \mathrm{I_M}) = \frac{\mathrm{GI}(\mathrm{I_M}, \mathrm{I_F})}{\mathrm{GI}(\mathrm{I_F}, \mathrm{I_F})}$$

where

$$\mathrm{GI}(\mathrm{p1}, \mathrm{p2}) = \sum_{\mathrm{i,j} \in \Omega} \mathrm{w(i,j)} \min\left(|\nabla \mathrm{p_1(i,j)}|, |\nabla \mathrm{p_2(i,j)}|\right),$$

$$\nabla \mathrm{p(i,j)} = \left(\frac{\mathrm{d}}{\mathrm{di}} \mathrm{p(i,j)} \frac{\mathrm{d}}{\mathrm{dj}} \mathrm{p(i,j)}\right),$$

and

$$\mathrm{w(i,j)} = \frac{1}{2}\left(\frac{\nabla \mathrm{p_1(i,j)} \nabla \mathrm{p_2(i,j)}}{|\nabla \mathrm{p_1(i,j)}||\nabla \mathrm{p_2(i,j)}|} + 1\right)$$

This paper only refers to Otake paper for robustness of this method without explanation.
Also, the CMA-ES optimizer was used to obtain the transformation that maximize NGI.

$$\widehat{\boldsymbol{T}_s}, \widehat{\boldsymbol{T}_\mathbf{d}}, \widehat{\boldsymbol{R}_\mathbf{d}} = \underset{\boldsymbol{T}_s, \boldsymbol{T}_\mathbf{d}, \boldsymbol{R}_\mathbf{d} \in \mathcal{S}}{\operatorname{argmax}} \mathrm{NGI}(I_\mathrm{F}, I_\mathrm{M}(\boldsymbol{T}_s, \boldsymbol{T}_\mathbf{d}, \boldsymbol{R}_\mathbf{d})).$$

Using this optimizer, the DRR and the projection image is down-sampled by a factor of 3 and population size was set to 100. Also, stopping criterion for this optimizer was set to be less than 0.1 mm translation and 0.1^o rotation. The maximum iteration is set to 10^6.
Then, using the resulting geometry of source and detector ($\mathrm{T_s}, \mathrm{T_d}$, and $\mathrm{R_d}$), PM is formed as

$$\boldsymbol{PM} := \begin{pmatrix} T_{s,z} & 0 & T_{s,x} & 0 \\ 0 & T_{s,z} & T_{s,y} & 0 \\ 0 & 0 & 1 & 0 \end{pmatrix} \begin{pmatrix} \boldsymbol{R_{3\times3}}(R_{\mathrm{d},x}, R_{\mathrm{d},y}, R_{\mathrm{d},z}) & \begin{matrix} T_{\mathrm{d},x} \\ T_{\mathrm{d},y} \\ T_{\mathrm{d},z} \end{matrix} \\ 0 \quad 0 \quad 0 & 1 \end{pmatrix},$$

It is noted that 3D-2D registration can be performed for either 6 or 9 DoF (and this paper discusses the different results using 6 DoF and 9 DoF later). An assumption that the source position $\mathrm{T_s}$ is fixed with respect to the detector reduces the system geometry from 9 DoF to 6 DoF.

Experimental Method

This paper conducts 4 experiments to measure performance of the self-calibration method. They use two system set-ups: a system with simple geometry and object (using the imaging bench and cylinder phantom) and a system with more complicated set-up (using the C-arm and head phantom) *(Figure 2)*.

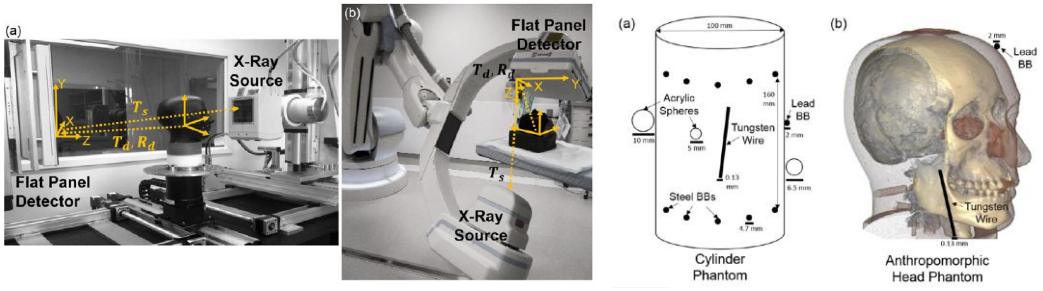

<Figure 2. Two system set-ups and phantoms>

Experiment 1 uses cylinder phantom on imaging bench. Experiment 2 uses head phantom on imaging bench. Experiment 3 uses head phantom on robotic C-arm. Experiment 4 uses non-circular orbit using imaging bench and head phantom.

This paper compares its self-calibration method to conventional 'Reference Calibration.' For the reference calibration of the bench system, the method of Cho *et al* (2005) is used and for the reference calibration of the Zeego C-arm, the method of Navab *et al* (1998) is used.

The performance is evaluated by several categories. The first measurement is the full-width at half-maximum (FWHM) of a point spread function (PSF) from the tungsten wire in each phantom. A Gaussian distribution is used to fit for each line profile and the FWHM is averaged over all line profiles. The second measurement is the reprojection error (RPE) from the position of the lead BB located on the surface of both phantoms. The centroid position of each 2D projection is transformed into 3D space using the PM and a line segment connecting these two points is generated. Repeating this process for all projections and taking the closest point of intersection yields a point cloud. The width of this point cloud is evaluated as RPE. The third category is to access image quality in terms of blur, noise, and artifacts from geometric calibration errors.

Result 1) Spatial Resolution (FWHM of the PSF)

This paper tests FWHM of the PSF about the tungsten wire for each experiment. The result is shown in the figure 3. For experiment 1 using cylinder phantom and the imaging bench, the PSFs are comparable with similar FWHM results (0.66 mm for self-calibration and 0.67 mm for reference calibration). Experiment 2 using head phantom and imaging bench shows improvement in FWHM (0.66 mm for self-calibration and 0.86 mm for reference calibration). Also, the general shape and intensity of PSF is improved for self-calibration method. For experiment 3 using head phantom and robotic C-arm, there is a measurable improvement of the PSF (FWHM) using self-calibration (0.55 mm for self-calibration and 0.73 mm for reference calibration). Experiment 4 using non-circular orbit with head phantom on imaging bench shows the feasibility of self-calibration for non-circular orbit as it gives same level of geometric accuracy in FWHM as for circular orbits in experiment 1 and 2 (Experiment 4 using self-calibration gives FWHM of 0.66 mm).

This paper hypothesizes the reasons for improvement of the PSF using self-calibration. They hypothesize that when the tungsten wire is further away from the isocenter (in the head phantom case), errors in detector angulations become more apparent using reference calibration. Also, an error in reference calibration might rise from the difference between the reference calibration and the current scan due to irreproducibility of the C-arm orbit.

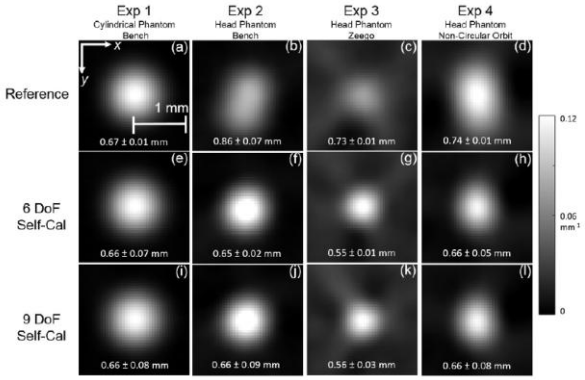

<Figure 3. Spatial Resolution (FWHM of the PSF>

Result 2) RPE (Reprojection Error)

Point cloud is generated using intersections of line segments which connect the centroid of BB in 2D projection and 3D location of BB. RPE is calculated as the width of the point cloud for each experiment.

For experiment 1 using cylindrical phantom and imaging bench, they observe a statistically significant improvement in RPE (0.69 mm for self-calibration and 0.83 mm for reference calibration with $p < 0.001$).

For experiment 2 using head phantom and bench, 6 DoF self-calibration method shows significant improvement in RPE compared to reference calibration (0.61 mm for 6 DoF self-calibration and 0.84 mm for reference calibration with $p < 0.001$). However, 6 DoF self-calibration method also shows significant improvement compared to 9 DoF self-calibration method. This paper discusses the reason for this counterintuitive result. They claim that 9 DoF method allow potentially unrealistic variations in source position with respect to the detector, possibly excursion along $T_{s,z}$.

For experiment 3 using head phantom and robotic C-arm, the mean and median RPE values are lower for

self-calibration method compared to the reference calibration but the difference is not statistically significant as p = 0.08. Error might be due to finding the BB centroid in the projection images and C-arm trajectory that deviates from a circular orbit.

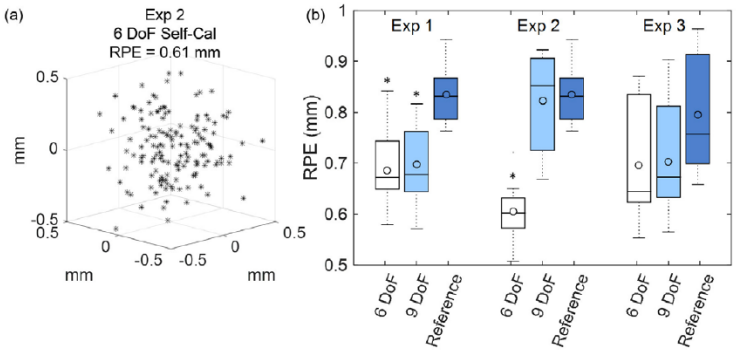

<Figure 4. a) an example of point cloud for RPE generation b) comparison of RPE for each experiment>

Result 3) Image Quality

Experiment 1 (data not shown) shows essentially identical images between using reference calibration and self-calibration. This is due to a simple object (cylinder phantom) without appreciable geometric artifacts.

Experiment 2 shows a qualitatively accurate reconstruction of the skull using both reference and self-calibration.

Experiment 3 manifests noticeable improvement in reconstruction of the skull using self-calibration. Reduction in streak artifact from the high-contrast biopsy needle is evident using self-calibration methods.

Experiment 4 shows a saddle orbit for self-calibration and a circular orbit (same as experiment 2) for reference calibration. The results show qualitatively identical image reconstruction using both self-calibration and reference-calibration. This shows the feasibility to compute a geometric calibration for non-circular orbit using self-calibration method.

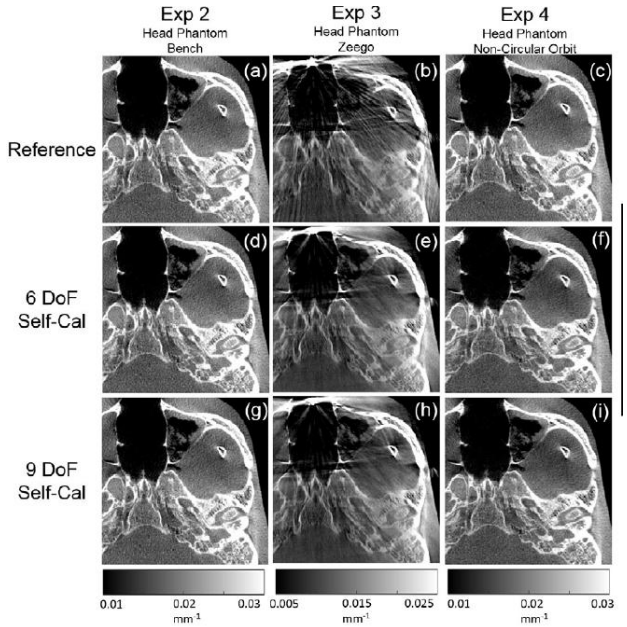

<Figure 5. Image quality comparison between self-calibration and reference-calibration>

Discussion / Assessment

This paper proposes a geometric calibration method not only for circular orbits and well calibrated systems but also for non-circular orbits and systems for which system geometry is irreproducible or unknown.

System set-ups from simple object (cylindrical phantom) to complicate object (head phantom) using bench imaging system and robotic C-arm are explored for performance measurements of self-calibration method. The results show comparable or improved results in terms of FWHM, RPE, and image quality compared to reference calibration. It is interesting to see that non-circular orbit can be geometrically calibrated using self-calibration method. However, they only provide qualitative support using FWHM and image quality to validate self-calibration for non-circular orbits. More quantitative results to support the accuracy of self-calibration for non-circular orbits will be helpful and interesting. Also, they do not mention the run-time of the algorithm for a complete scan. If this self-calibration method is to be used during clinical surgeries, their run-time should be optimized and they mention optimizing run-time as their future steps in their discussion. They refer other papers such as Otake *et al* (2012, 2013) to explain their technical approach (3D-2D image registration). It would have been helpful if they explain more about equations mentioned in the paper.

Conclusion

In conclusion, this paper provides a good possible method for 3D-2D image registration for out project as one of our maximum deliverables is patient-CT 3D-2D registration. Since our C-arm can make oblique movement, where trajectory is not circular, this self-calibration method can be applicable. If this method is applied in our project, we will be able to not only get rid of optical tracking of patient but also provide robust, reliable geometric calibration of any C-arm movement.

Reference

[1] Ouadah, S., J. W. Stayman, G. J. Gang, T. Ehtiati, and J. H. Siewerdsen. "Self-calibration of Cone-beam CT Geometry Using 3D–2D Image Registration."Physics in Medicine and Biology Phys. Med. Biol. 61.7 (2016): 2613-632. Web.